



Gopi, S, Mohan, Dhanesh G and Natarajan, Elango (2023) Mechanical and Corrosion Properties of Friction Stir Welded and Tungsten Inert Gas Welded Phosphor Bronze. *Advances in Materials Science*. ISSN 2083-4799

Downloaded from: <http://sure.sunderland.ac.uk/id/eprint/17706/>

Usage guidelines

Please refer to the usage guidelines at <http://sure.sunderland.ac.uk/policies.html> or alternatively contact sure@sunderland.ac.uk.

S. Gopi¹, Dhanesh G. Mohan^{2*}, Elango Natarajan³

¹*Department of Production Engineering, Government College of Technology, Coimbatore, Tamilnadu, India*

²*Zhengzhou Research Institute, Harbin Institute of Technology, Zhengzhou, Henan, China*

³*Faculty of Engineering, Technology and Built Environment, UCSI University, Kuala Lumpur, Malaysia*

*dgmohan@hit.edu.cn

MECHANICAL AND CORROSION PROPERTIES OF FRICTION STIR WELDED AND TUNGSTEN INERT GAS WELDED PHOSPHOR BRONZE

ABSTRACT

This study investigated the mechanical and corrosion properties of Friction Stir Welded (FSW) and Tungsten Inert Gas (TIG) welded phosphor bronze (CuSn4) joints. Corrosion tests were conducted on the welded joints, and the percentage of weight loss due to corrosion was measured at different time intervals. Results revealed that the percentage of weight loss due to corrosion of the TIG joint increased with time, whereas the percentage of weight loss due to corrosion of the FSW welded joint remained constant. This could be attributed to recrystallisation that happened in the solid-state welding, which reduced corrosion in the FSW welded joint. In addition, tensile tests were conducted to evaluate the strength of the joints. FSW with a spindle speed of 1300 rpm, weld speed of 0.06mm/sec, plunge depth of 0.25mm, pin profile of pentagon, and flat shoulder profile was found to produce good results. TIG welding with a welding speed of 1.75mm/sec, a gas flow rate of 7.5 cm³/min and an amperage of 120A also produced good results. The tensile strength of FSW was found to be approximately 1.6 times higher than that of TIG welding.

Keywords: friction stir welding; tig; phosphor bronze; corrosion; tensile strength; welding

INTRODUCTION

Prosper Bronze, a specialised bronze alloy, finds widespread use due to its unique combination of properties. High strength and hardness make it suitable for structural components subjected to heavy loads. Its corrosion resistance makes it ideal for marine equipment and plumbing systems [1]. Prosper Bronze's wear resistance makes it suitable for bearings and gears, while its excellent machinability allows for easy shaping. It also exhibits good thermal and electrical conductivity, making it useful in heat exchangers and electrical connectors. Prosper Bronze's diverse range of properties makes it a favoured choice across industries for applications requiring strength, corrosion resistance, wear resistance, machinability, and aesthetic appeal [2].

Friction Stir Welding (FSW) has emerged as a highly promising solid-state joining

technique for welding Phosphor Bronze, offering significant advantages over traditional fusion welding methods. By operating below the melting temperature of the materials, FSW ensures the retention of the desired properties of Phosphor Bronze [3]. This autogenous and continuous process involves the use of a non-consumable spinning tool with a harder surface than the Phosphor Bronze being welded, generating frictional heat and mechanical stirring for effective material joining [4,5]. FSW presents several notable benefits when applied to Phosphor Bronze welding. Firstly, it eliminates common issues encountered in fusion welding, such as oxidation and porosity. By operating in the solid state, FSW minimises the exposure of Phosphor Bronze to oxygen, preventing the formation of detrimental oxide layers and porosity. As a result, high-quality welds with improved integrity and reduced defects can be achieved. Furthermore, FSW enables precise control over the heat input during the welding process, minimising distortion and preserving the mechanical properties of the Phosphor Bronze [6]. The absence of filler metals simplifies the welding process and reduces material costs, while the mechanical stirring action promotes the homogenisation of the material, enhancing joint strength and integrity [7-9].

The advantages of FSW for welding Phosphor Bronze make it an attractive alternative to fusion welding methods in various applications. The solid-state nature of FSW ensures the preservation of the material's properties, offering better control over the heat-affected zone and minimising thermal distortion. Furthermore, the absence of fusion-related defects, such as solidification cracks, contributes to the overall reliability and durability of the weld joint [10]. These benefits are particularly advantageous for Phosphor Bronze, a material known for its unique mechanical and corrosion-resistant properties. The elimination of common issues associated with fusion weldings, such as oxidation and porosity, leads to high-quality welds with improved structural integrity and reduced vulnerability to corrosion [11,12]. Overall, the application of FSW in Phosphor Bronze welding offers significant potential for enhancing the performance and reliability of welded components in various industries.

The Tungsten Inert Gas (TIG) welding process is widely employed for various applications, including the welding of Phosphor Bronze. However, the welding of Phosphor Bronze using TIG poses several challenges and potential problems that need to be addressed. Oxidation is a significant concern during the TIG welding of Phosphor Bronze due to its susceptibility to oxidation at elevated temperatures [13-15]. The formation of oxide layers on the weld surface can negatively impact the weld quality and integrity. Proper cleaning procedures and careful selection of shielding gases are crucial to minimising oxidation effects. Another challenge lies in controlling the heat input during TIG welding, as excessive heat can lead to distortion, warping, and overheating of the base metal, compromising the structural integrity of the weld joint [16]. Skilled welders are required to manage heat input effectively and maintain the desired weld quality.

Precise joint fit-up is critical to the successful TIG welding of Phosphor Bronze. Accurate alignment and tight fit-up of the joint are essential for uniform heat distribution and proper fusion. Poor joint fit-up can result in inadequate weld quality, including lack of fusion or incomplete penetration. Additionally, weld cracking is a common issue encountered in Phosphor Bronze welding. Both hot cracking and solidification cracking pose risks during the welding process [17]. Hot cracking can occur due to the material's high thermal expansion and contraction rates, while solidification cracking can manifest during the cooling phase of the weld. Employing appropriate welding techniques, selecting suitable filler metals, and implementing preheating and cooling methods can help mitigate these cracking issues. Furthermore, careful selection of filler metals is crucial to ensure compatibility with Phosphor Bronze, as improper filler metal choices can lead to reduced weld strength, diminished corrosion resistance, or base metal incompatibility [18,19]. Post-weld cleaning procedures are

also essential to remove residual flux, slag, and oxides, which can compromise joint integrity, corrosion resistance, and aesthetics.

Effectively addressing these challenges and mitigating the potential problems associated with TIG welding of Phosphor Bronze requires a combination of skilled welders, proper equipment setup, meticulous joint fit-up, suitable filler metal selection, and thorough post-weld cleaning procedures. By overcoming these obstacles, high-quality TIG welds can be achieved in Phosphor Bronze, ensuring the integrity and performance of welded components in various applications [20].

In the welding process, distinct zones, namely the weld nugget, heat-affected zone (HAZ), and parent material, are typically observed surrounding the welded area. However, in Friction Stir Welding (FSW), an additional zone known as the thermo-mechanically affected zone (TMAZ) is identified between the weld nugget, the stirred zone, and the HAZ. Figures 1(a) and 1(b) provide schematic representations of different FSW and TIG weld zones [21,22].

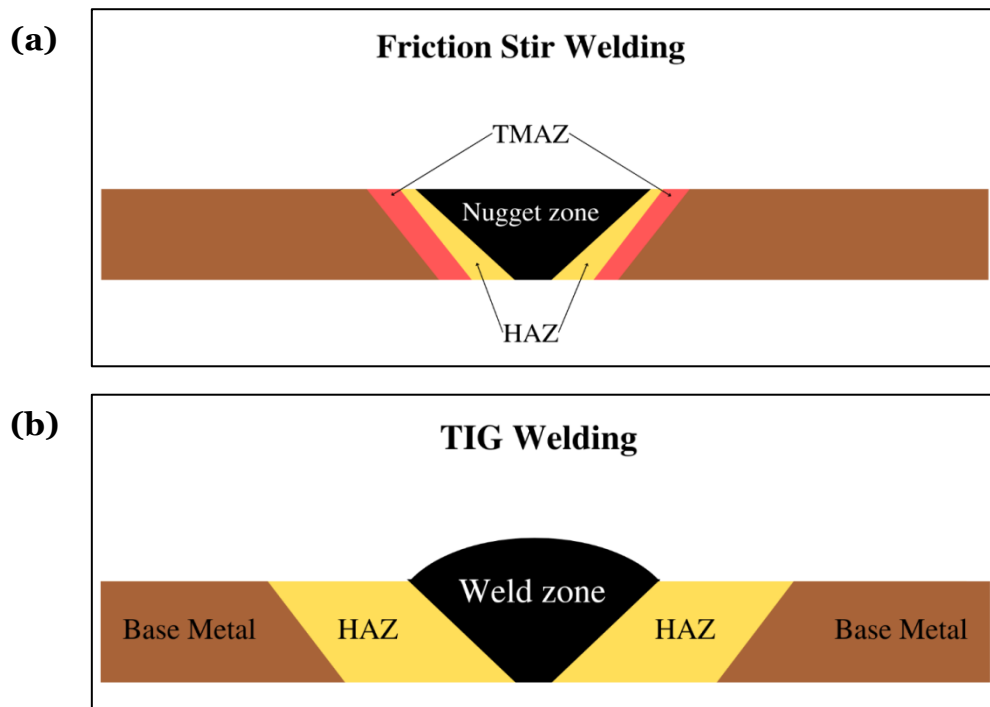


Fig. 1. (a) Weld zones of FSW, (b) weld zones of TIG

Moreover, FSW exhibits two distinct zones on each side of the joined materials, dependent on the direction of the tool travel and rotational movement. The side where the tool travel and rotational directions align is referred to as the advancing side (AS), while the side where the tool travel and rotational directions oppose each other is termed the retreating side (RS). This disparity in the tool's travel and rotation creates a temperature gradient, resulting in higher temperatures on the advancing side compared to the retreating side [23]. Consequently, when welding dissimilar materials using FSW, it is recommended to position the weaker material on the advancing side to optimise the welding outcome.

V. Shokri et al. conducted a comparative study on friction stir welded (FSWed) and Tungsten Inert Gas (TIG) welded joints of DSS-Cu to assess their respective characteristics [24]. The results indicated that FSWed joints exhibited superior strength when compared to

fusion welded joints. This can be attributed to the precise and reformed microstructure observed in FSWed joints. The refined grain structure effectively impeded crack formation and increased the tensile strength of the joints. Conversely, the TIG samples demonstrated poor mechanical properties, mainly due to excessively high heat inputs, resulting in the formation of a thick-phase layer that concentrated stress along the weld line. The low heat inputs during FSW also led to inadequate plasticisation and mixing, resulting in poor welding quality.

In another investigation by A. Squillace et al., a comparison was made between FSWed and TIG welded AA 2024-T3 alloy plates in terms of their mechanical and corrosion properties [25]. The FSWed joints exhibited a slight recovery in the nugget zone, owing to their extremely fine grain structure, while the heat-affected zone (HAZ) showed only a minor decline in mechanical properties. Microhardness tests conducted across the thickness of the TIG weld joint confirmed the overall deterioration in mechanical characteristics observed in both the weld bead and HAZ, attributed to phase transitions induced by high temperatures experienced during the welding process [26, 27]. Both the FSWed and TIG joints exhibited passive behaviour in the weld bead and HAZ; however, the parent alloy demonstrated a propensity for pitting, as evidenced by the polarisation curve and electrochemical impedance spectroscopy (EIS) tests, although this tendency was less pronounced in FSW joints. Comparisons between the advancing and retreating sides of the friction stir weld bead provided some indication of the nobler behaviour exhibited by the latter zone.

A comprehensive investigation by Srinivasa Rao et al. examined the mechanical properties and microstructure of 5 mm thick plates made of Al-4.2Mg-0.6Mn-0.4Sc-0.1Zr alloy [28]. The plates were subjected to two welding procedures: friction stir welding (FSW) and tungsten inert gas (TIG) welding. The study revealed a notable reduction in strength for the TIG welded joint compared to the FSW welded joint. The FSW process induced fine-grain refinement in the stir zone of the Al-4.2Mg-0.6Mn-0.4Sc-0.1Zr alloy, leading to enhanced material strength. Consequently, the FSW welded joint achieved a joint efficiency of 91.6%, surpassing the TIG welded joint's efficiency of 69.8%.

After friction stir welding, the resulting Al-4.2Mg-0.6Mn-0.4Sc-0.1Zr alloy exhibited the following mechanical properties: hardness (118.98 VHN), ultimate tensile strength (238.54 MPa), bending strength (3325 MPa), impact strength (11.25 KJ/m²), and elongation percentage of 4.9. The friction stir welded alloy demonstrated significant improvements, achieving 85.5% hardness, 91.6% ultimate tensile strength, 95.5% bending strength, 24.8% impact strength, and an elongation percentage of 66.2% when compared to the non-welded Al-4.2Mg-0.6Mn-0.4Sc-0.1Zr alloy. On the other hand, the TIG welded Al-4.2Mg-0.6Mn-0.4Sc-0.1Zr alloy exhibited the following mechanical properties: hardness (94 VHN), ultimate tensile strength (157.86 MPa), bending strength (3215 MPa), impact strength (3.8 KJ/m²), and elongation percentage of 4.6. Comparatively, the TIG welded alloy achieved 32.3% hardness, 39.3% ultimate tensile strength, 7.6% bending strength, 24.8% impact strength, and an elongation percentage of 66.2% when compared to the non-welded Al-4.2Mg-0.6Mn-0.4Sc-0.1Zr alloy [29, 30]. These findings highlight the significant advantages of friction stir welding in terms of improved mechanical properties and performance of the Al-4.2Mg-0.6Mn-0.4Sc-0.1Zr alloy compared to TIG welding and the non-welded state.

The existing literature emphasizes the investigation of many aspects related to Friction Stir Welding, such as parameters and tool profiles, their effects on fatigue and tensile characteristics, and microstructure development. Comparative studies between tungsten inert gas (TIG) welding and friction stir welding have also received much interest, particularly regarding alloy systems other than aluminium [31]. These questions shed light on the differences between FSW and TIG welding processes, highlighting the benefits of FSW over

conventional fusion welding in terms of increased strength, accurate microstructure, and less vulnerability to pitting corrosion.

This study mainly highlights the investigation of many aspects related to Friction Stir Welding, such as parameters, tool profiles, and their influence on fatigue and tensile characteristics as well as microstructure development. Furthermore, a great deal of focus has been placed on comparing studies between tungsten inert gas (TIG) welding and friction stir welding, particularly with regard to aluminium and other alloy systems [31]. These questions highlight the differences between FSW and TIG welding processes, whereby FSW is superior to conventional fusion welding in terms of strength, microstructure accuracy, and reduced vulnerability to pitting corrosion.

MATERIALS AND METHODS

The material under investigation in this study is phosphor bronze, specifically CuSn4 alloy. Plate specimens with dimensions of 4mm thickness, 100mm length, and 50mm width were selected for friction stir welding (FSW) and tungsten inert gas (TIG) welding. Simple butt weld joints were fabricated along the lamination direction under ambient conditions [32]. The chemical compositions and mechanical properties of the specimens provided by the supplier are presented in Tables 1 and 2, respectively.

Table 1. Chemical compositions of CuSn4, wt. %

Cu	Sn	Zn	Fe	P	Ni	Si	Mn
95.75	4.02	0.109	0.0253	0.620	0.017	0.052	0.0066

Table 2. Mechanical properties of CuSn4

Density	8.86 gm/cm ³
Elastic Modulus	101.7 N/mm ²
Tensile Strength	483.3 MPa
Yield Strength	462.5 MPa
Elongation	2%
Hardness	121 BHN

Prior to the welding process, the butting surface of the metals was cleaned using an acetone solution, ensuring a clean and suitable surface for the welding operation. A custom-designed clamping fixture was employed to securely affix the two plates during FSW and TIG processes to ensure precise and controlled welding operations [33]. This clamping fixture facilitated optimal alignment and stability of the plates throughout the welding procedures.

Tungsten inert gas (TIG) welding was conducted using direct current single polarity

(DCSP) from a power source characterised by drooping V-I static characteristics. A tungsten electrode of type A 203, typically sharpened to a cone angle of 60° with a flat tip ranging from 0.125 to 0.50mm, was employed [34]. The machine used for the TIG operation is a DC inverter TIG welder (model: PI 180 MT, manufacture: Powercon Electronics, Amperage range - 10-180 A, welding rods - Phosphor bronze). In the case of square butt joints in copper alloys up to 3mm thick, no filler metal was necessary. However, since a plate with a thickness of 4mm was utilised in this study, a filler material containing residual deoxidisers was employed to mitigate the adverse effects of oxygen on the welded joint [35]. Specifically, a filler rod with the same composition as the base metal, including a maximum of 0.15% phosphorus, was employed for the TIG welding process.

The FSW operations were performed on a vertical milling machine (model: FN2 - knee type milling machine, speed range: 35.5-1800 rpm and number of feeds: 18), providing a stable and controlled platform for the welding process. A non-consumable carbide tool with a pin length of 3.4mm, a pin diameter of 2.5mm with a pentagonal profile and a shoulder diameter of 25mm with a flat face is adopted for this work [36-39]. The pentagonal profile provides maximum distortion in the stir zone and will help attain a refined grain structure. To maintain consistency and minimise potential variations, a single-pass welding technique was employed to fabricate the joints, ensuring uniformity and enabling reliable analysis of the resulting weld characteristics [40]. The process parameters are finalised after conducting trial runs and a literature review. In this work, the welding current for TIG welding is kept constant, and in FSW, the plunge depth is kept constant. The process parameters selected for TIG and FSW are given in Table 3.

Table 3. TIG and FSW process parameters

TIG Welding			
Sl. No.	Welding Current (A)	Welding Speed (mm/s)	Gas flow rate (cm ³ /min)
T1		1.45	5
T2	120	1.95	7.5
T3		2.45	10
FSW			
Sl. No.	Spindle Speed (rpm)	Welding Speed (mm/s)	Plunge depth (mm)
F1	1200	0.02	
F2	1300	0.06	0.25
F3	1400	0.10	

The TIG and FSW joints were carefully sectioned in the transverse direction to obtain representative specimens for analysis. The sectioning process involved cutting along the welding direction, effectively separating the weld bead and the heat-affected zone (HAZ) from the parent alloy. In order to conduct corrosion testing, the specimens were embedded in epoxy resin, ensuring that only the welded surface was exposed to the salt solution, thereby facilitating an accurate assessment of the corrosion behaviour [41]. To prepare the FSW and TIG welded specimens for further analysis, a thorough cleaning process was carried out. The specimens were initially cleaned using emery papers up to a grit size of 1000, ensuring the removal of any surface impurities or irregularities. Subsequently, the specimens were washed with distilled water to eliminate any residual contaminants [42]. Finally, a degreaser was

applied to achieve a smooth and pristine surface, ready for subsequent characterisation and evaluation. Tensile and bend tests were conducted for all the weldments made with the optimised input variables following ASTM E8 and E190-14 standards. Figure 2 (a) shows the FSW sample specimens, and Figure 2(b) shows the TIG sample specimens for tensile testing.

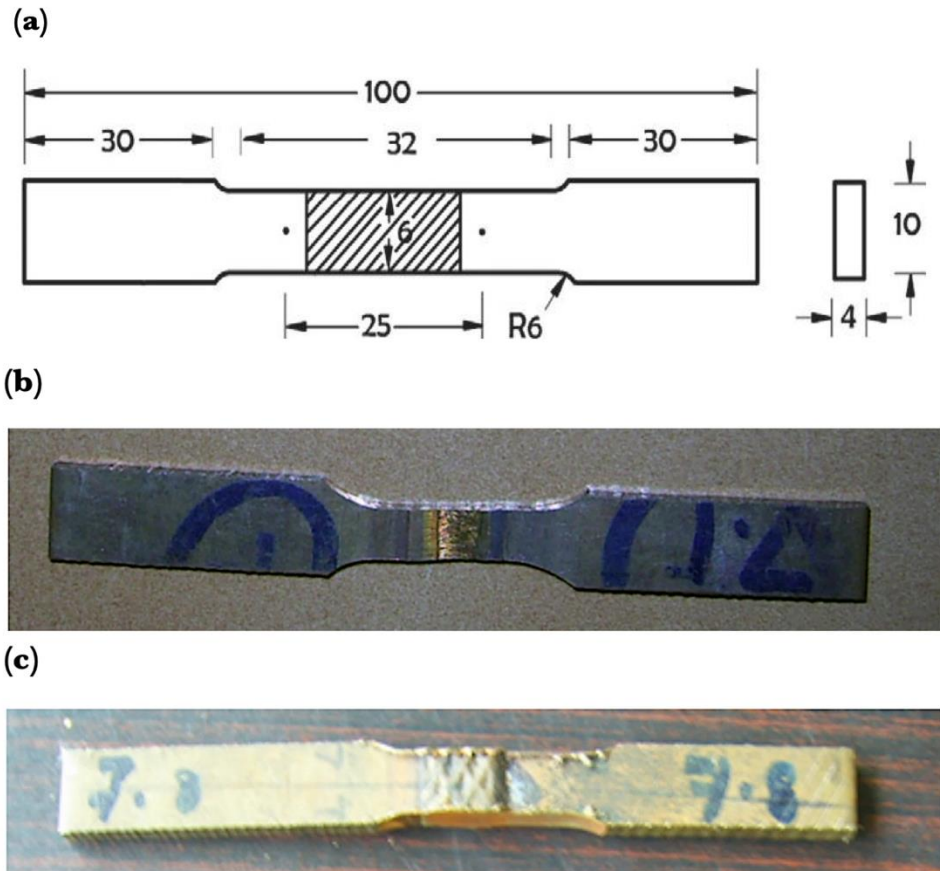


Fig. 2. (a) Tensile test specimen dimensions (b)FSW sample specimen (c) TIG sample specimen

The weight loss corrosion test was conducted per ASTM G31 standards. After cleaning, the metal samples are blow-dried and weighed. The gravimetric measurements were made by using a precision balance (with a range of 41/120 g and an accuracy of $\pm 0.01/0.1$ mg). These readings correspond to the mass of the specimen before welding [43,44].

After initial weighing of all the TIG and FSW samples, they were suspended, and the weld zones were immersed into 500ml beakers containing 3.5wt % sodium chloride solution separately at room temperature. Figure 3 shows the specimens immersed in 3.5wt % sodium chloride solution [45], except for the weld region; all the other areas of the weldments were coated with transparent epoxy to attain accurate results. This solution has a neutral pH with the composition of sodium chloride equal to the seawater composition. Since phosphor bronze has major applications in marine areas, corrosion testing was carried out in this environment [46,47].

Since a pair of pieces were machined from each welded joint, one among the pairs was taken out after 168 hours. These pieces were analysed individually. These samples were then flushed with water and immersed into the solution of 500ml Hydrochloric acid (density 1.19) +1000 ml distilled water for two minutes to clean off the corrosion products [48]. Then the samples are completely rinsed out using a brush and flushed with water. Finally, the samples are immersed in ethyl alcohol, blow-dried, and weighed.

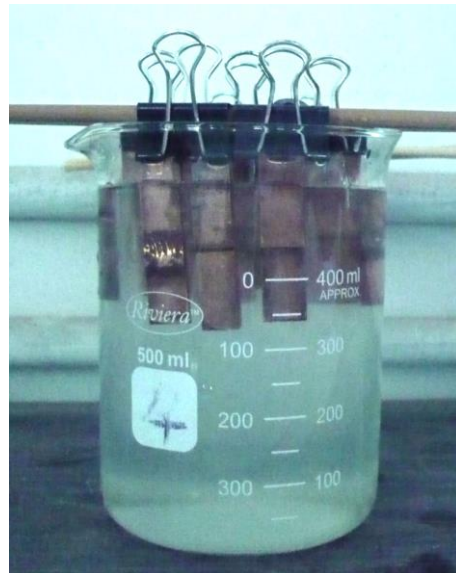


Fig. 3. Specimens immersed in 3.5wt % sodium chloride solution

RESULTS AND DISCUSSION

In Tungsten Inert Gas (TIG) welding, a recognised phenomenon emerges due to the fusion of materials and the elevated temperatures affecting nearby substances. As Figure 4 illustrates, this process results in the formation of a larger Heat-Affected Zone (HAZ) compared to FSW weldment. In this heat-affected zone, the primary hardening precipitates ageing excessively, causing ensuing phase changes that lead to a discernible deterioration in their overall mechanical characteristics [49-51]. The results obtained from the investigation into the Tungsten Inert Gas (TIG) welding and Fabricated Friction Stir Welding (FSW) joints reveal intriguing insights into the structural, mechanical, and corrosion aspects of the welded specimens.

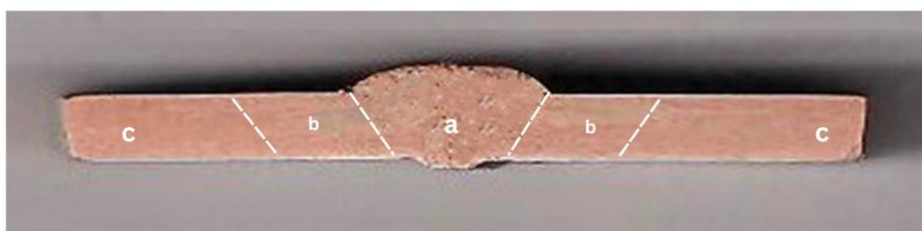


Fig. 4. TIG- Specimen, a. Fusion zone, b. Heat-affected zone, c. Base metal

In the context of Fabricated Friction Stir Welding (FSW) joints, it is imperative to address two distinct phenomena, each leading to disparate outcomes. Firstly, the temperatures endured by the materials involved in the welding procedure, albeit lower than their melting points, instigate phase transformations akin to those exhibited in TIG joints [52]. Consequently, the mechanical properties deteriorate, encompassing the nugget, Thermal-Mechanically Affected Zone (TMAZ), and Heat-affected zone (HAZ), as depicted in Fig. 5.

These temperature-induced phase changes intricately influence the material's structure, leading to alterations in its mechanical behaviour. Understanding this thermal-mechanical interplay is vital as it provides valuable insights into the challenges inherent in Fabricated Friction Stir Welding. Figure 5 emphasises the distribution of these effects, offering a comprehensive view of the regions impacted by welding-induced temperature changes. The nuanced relationship between heat and material characteristics holds significance in optimising the FSW process within the broader context of welding techniques. This sets the stage for a deeper exploration of the intricate connections shaping the mechanical properties of FSW joints, underscoring the importance of addressing specific thermal phenomena for improved accuracy and control in welding operations.

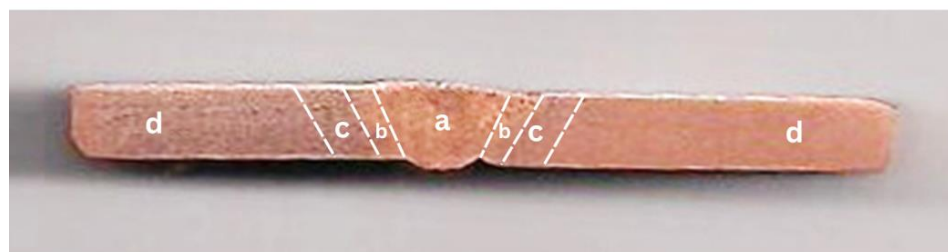


Fig. 5. FSW specimen, a. Nugget zone, b. Thermo mechanical affected zone, c. Heat-affected zone, d. Base metal

Secondly, the substantial shear stresses induced by the motion of the welding tool facilitate the formation of an exceptionally fine-grained microstructure. This outcome, primarily observed in the nugget zone and predominantly in the flow arm zone, permits a partial restoration of mechanical properties [53,54]. A distinct pattern emerges as one traverses from the central axis of the weld bead towards the base material, traversing the TMAZ and transitioning into the HAZ. Within this region of FSW joints executed on phosphor bronze alloys akin to those under scrutiny in this present study, exemplified by the F2 sample, the relatively lower temperatures encountered can induce a form of ageing [55]. This ageing effect yields a modest augmentation in mechanical characteristics.

The mass of the specimens before and after corrosion for both the FSW and TIG welded joints with corresponding % of weight loss are given in Table 4. The percentage of weight loss due to corrosion is calculated by using the following formula [56].

$$\% \text{ of weight loss} = \frac{\text{Mass of the weld before corrosion} - \text{Mass of the weld after corrosion}}{\text{Mass of the weld specimen before corrosion}}$$

The mass of the welds before corrosion and after corrosion are measured. The ratio of the difference between the corroded samples and the parent welds to the mass of the parent weld gives the percentage of corrosion that has occurred.

The findings presented in Table 4 provide valuable insights into the corrosion behaviour of the investigated specimens. Notably, the extent of weight loss attributed to corrosion is markedly lower in Friction Stir Welded (FSW) samples as compared to those subjected to Tungsten Inert Gas (TIG) welding, as evidenced by the data obtained over a 7-day analysis period.

Table 4. Mass of the specimens before and after corrosion with % of weight loss

FSW			
Specimens	Mass before corrosion (g)	Mass after corrosion (g)	% of weight loss due to corrosion
F1	17.167	17.153	0.081
F2	19.566	19.553	0.066
F3	17.244	17.228	0.092
TIG			
Specimens	Mass before corrosion (g)	Mass after corrosion (g)	% of weight loss due to corrosion
T1	19.400	19.351	0.252
T2	18.400	18.360	0.217
T3	19.168	19.124	0.229

Specimen F2, a representative of the FSW welds, exhibited an impressively minimal weight loss of 0.066%, indicating high corrosion resistance. In contrast, specimen T2 displayed the most favourable corrosion resistance among the TIG-welded specimens, with a weight loss of 0.217%. However, it is noteworthy that even the best-performing TIG-welded specimen still demonstrated a corrosion weight loss that was 3.4 times greater than that of the FSW specimen (F2). Corrosion properties are inherently influenced by a multitude of factors, encompassing temperature, the concentration of corrosive agents, diffusion rates, and the presence of oxidising agents, among others [57]. These factors collectively dictate the susceptibility of the materials to corrosion processes. Beyond these well-established influences, the corrosion resistance of metals is also intricately linked to microstructural characteristics.

Particularly, the grain size and the presence of precipitated particles can significantly impact the corrosion properties of the materials. A finer grain structure, often attainable through the unique thermomechanical conditions of FSW, can contribute to enhanced corrosion resistance due to the reduced presence of grain boundaries and potential preferential sites for corrosion initiation [58,59]. Furthermore, the influence of precipitated particles, including second-phase particles and precipitates formed during the welding process, cannot be understated. Such particles can influence local electrochemical behaviour, altering the corrosion susceptibility of the material. The synergistic effects of grain size refinement and precipitate formation in FSW-welded materials could contribute to the superior corrosion performance observed in specimen F2 [60].

In contrast, the data from Table 4 underscores the remarkable corrosion resistance exhibited by the Friction Stir Welded specimens, particularly exemplified by specimen F2, as compared to their TIG-welded counterparts. While factors such as temperature and chemical environment remain significant drivers of corrosion, the role of microstructural attributes, specifically grain size and precipitate presence, should not be underestimated [61, 62]. This comprehensive understanding of corrosion behaviour is pivotal in guiding the optimisation of welding processes for improved material performance and longevity in corrosive environments.

All experimental trials involving friction stir and TIG welding were meticulously executed under controlled ambient conditions, maintaining a temperature range of 23°C to 27°C and a dynamic relative humidity fluctuation spanning from 15% to 20%. Within the context of the FSWed specimen, a notable thermal dichotomy is observed, with the advancing side (AS) exhibiting heightened heat generation compared to the retreating side (RS) [63]. This phenomenon is attributed to the rotational motion of the tool, effectively transporting cooler material from the AS to the RS. Consequently, when effecting the fusion of phosphor

bronze, strategic placement of the alloy material at the RS is employed to harness enhanced strength generation at the AS, thereby augmenting the comprehensive mechanical robustness of the welded interconnections. Figure 6 is a graphic representation of the average strength attributes of butt joints made of phosphor bronze using both FSW and TIG welding processes [64].

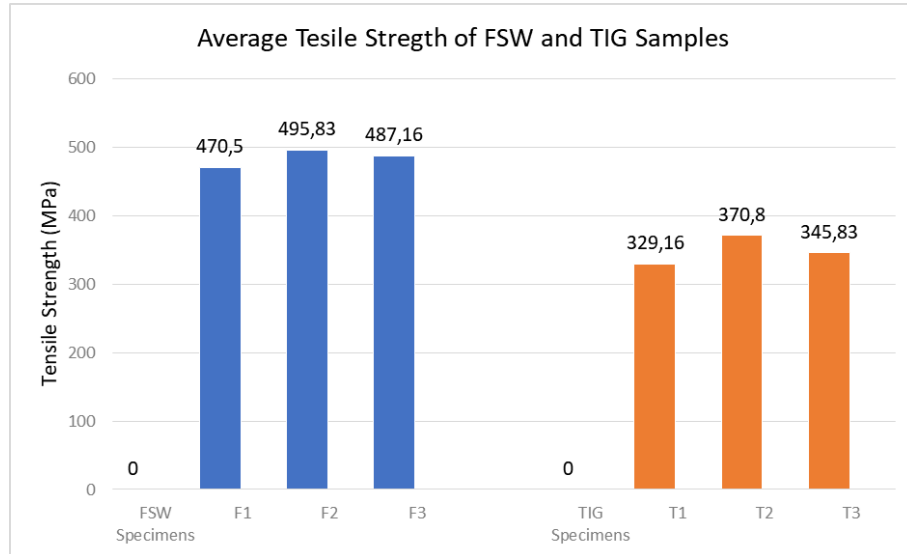


Fig. 6. Average tensile strength of FSW and TIG specimens

Additionally, Figure 6 provides a comparative analysis between the FSWed joint and the TIG welded joint, predicated upon the outcomes of meticulously conducted tensile tests. Among the FSWed specimens, Sample F2 stands out as possessing the most elevated joint tensile strength. This pinnacle achievement was realised through the implementation of specific parameters, specifically a tool rotation rate of 1300 rpm, welding speed of 0.06 mm/s, and a plunge depth of 0.25 mm. Sample F2 exhibited an average tensile strength of 495.83 MPa. In contrast, the tensile strength attained through the TIG welded connection was comparatively diminished [65, 66]. It can be clearly seen in Figure. 6 that FSWed joints display tensile strength almost 1.6 times higher when compared to TIG welded joints.



Fig. 7. (a) FSW specimen, (b) TIG Specimen, after tensile testing

Figure. 7 a and b show that the FSW joint failed in AS of the SZ during tensile tests, while the TIG joint failed in the welded zone.

CONCLUSIONS

The comparative results between the FSW and TIG welding on phosphor bronze show that:

- The tensile strength of FSW joints is comparatively higher than that of TIG welded joints. The F2 specimen prepared by the FSW method exhibits the highest average tensile strength of 495.83 MPa, where the highest tensile strength provided by the TIG joint T2 is 370.8 MPa.
- The percentage of weight loss of the FSW specimen is 0.066%, and the TIG specimen is 0.217%. This means the FSW specimen is 3.4 times better corrosion-resistant than the TIG specimen.

The experimental analysis reveals that FSW provides higher quality butt welded joints for phosphor bronze than TIG. FSW creates higher-quality welds since it is a solid-state method that does not modify the mechanical properties of the parent material. Furthermore, the dynamic recrystallisation of the grains in the weld or stirring zone produces a high-quality weld with improved tensile performance.

REFERENCES

1. Hu D, Chen M, Wang L, Cheng H: Dynamic tensile behaviour and deformational mechanism of C5191 phosphor bronze under high strain rates deformation. *Materials Science and Engineering: A*, 2016, 649, 68–73.
2. Sanga B, Wattal R, Nagesh D S: Weld joint characterization in ultrasonic welding of phosphor bronze sheets. *Engineering Science and Technology, an International Journal*, 2022, 30, 101040.
3. Velu M, Bhat S: Experimental investigations of fracture and fatigue crack growth of copper–steel joints arc welded using nickel-base filler. *Materials & Design*, 2015, 67, 244–260.
4. Makeshkumar M, Surender S R, Arunprakash S, Madesh R, Sasi Kumar M, Sudharsan K: Microstructural and mechanical properties evaluation of dissimilar aluminum alloy and bronze joints using friction stir welding. *Materials Today: Proceedings*, 2021, 47, 5239–5244.
5. Chaudhary V, Bharti A, Azam S M, Kumar, N, Saxena K K: A re-investigation: Effect of TIG welding parameters on microstructure, mechanical, corrosion properties of welded joints. *Materials Today: Proceedings*, 2021, 45, 4575–4580.
6. Mohan D G, Tomków J, Gopi S: Induction Assisted Hybrid Friction Stir Welding of Dissimilar Materials AA5052 Aluminium Alloy and X12Cr13Stainless Steel. *Advances in Materials Science*, 2021, 21(3), 17–30.
7. Zoeram A S, Anijdan S H M, Jafarian H R, Bhattacharjee T: Welding parameters analysis and microstructural evolution of dissimilar joints in Al/Bronze processed by friction stir welding and their effect on engineering tensile behavior. *Materials Science and Engineering: A*, 2017, 687, 288–297.
8. Mohan D G, Wu C: A Review on Friction Stir Welding of Steels. *Chinese Journal of Mechanical Engineering*, 2021, 34(1), 137.
9. Rabiezadeh A, Salafzon A, Mostafavi N: Dissimilar welding of AA5083/AA7039 by self-reacting friction stir welding. *Journal of Adhesion Science and Technology*, 2023, 1–22, in Press.
10. A M, SS KV, A P K: On the friction stir welding of alloy AA2014 under n-MQL cooling condition. *Journal of Adhesion Science and Technology*, 2023, 37(13), 2025–2045.

11. Sasikumar A, Gopi S, Mohan D G: Prediction of Filler Added Friction Stir Welding Parameters for Improving Corrosion Resistance of Dissimilar Aluminium Alloys 5052 and 6082 Joints. *Advances in Materials Science*, 2022, 22(3), 79–95.
12. Yin, Cao L, Wang N: Mechanical properties and residual stresses of 5083 to AM60B dissimilar friction stir welding with different process parameters. *Journal of Adhesion Science and Technology*, 2019, 33(23), 2615–2629.
13. Anbalagan K, Ramasubramanian S, David C, Manivannan S, Kannan AR, Mohan DG: Importance of shielding and mechanical characterization of GTAW on Ti-6AL-4V alloy sheet. *Welding International*, 2023, 37(6), 324–333.
14. Chen X H, Ma YF, Cheng Y J, Wang Z D, Yang M, Jiang W W, Cao Y D: Strengthening and toughening strategies of weld metal for in-situ nanoparticle reinforced tin bronze alloy. *Science and Technology of Welding and Joining*, 2021, 26(4), 309–315.
15. N V Babu: Fatigue strength of welded joints in complexly alloyed aluminium bronzes. *Welding International*, 1989, 3(5), 386–388.
16. Cheng Z, Liu H, Huang J, Ye Z, Yang J, Chen S: MIG-TIG double-sided arc welding of copper-stainless steel using different filler metals. *Journal of Manufacturing Processes*, 2020, 55, 208–219.
17. Velu M, Bhat S: Metallurgical and mechanical examinations of steel–copper joints arc welded using bronze and nickel-base superalloy filler materials. *Materials & Design*, 2013, 47, 793–809.
18. Poggie R A, Wert J J, Harris L A: The effects of surface oxidation and segregation on the adhesional wear behavior of aluminum—bronze alloys. *Journal of Adhesion Science and Technology*, 1994, 8(1), 11–28.
19. Saraiva A S, Figueiredo E, Águas H, Silva R J C: Characterisation of Archaeological High-tin Bronze Corrosion Structures. *Studies in Conservation*, 2022, 67(4), 222–236.
20. C S Radhika, N Kumar, Sivasailam B: A review on welding techniques: properties, characterisations and engineering applications. *Advances in Materials and Processing Technologies*, 2023, 1(1), 1–56.
21. Nakata K: Friction stir welding of copper and copper alloys. *Welding International*, 2005, 19(12), 929–933.
22. Çam G: Friction stir welded structural materials: beyond Al-alloys. *International Materials Reviews*, 2011, 56(1), 1–48.
23. Mohan D G, Gopi S: Induction assisted friction stir welding: a review. *Australian Journal of Mechanical Engineering*, 2020, 18(1), 119–123.
24. Shokri V, Sadeghi A, Sadeghi M H: Effect of friction stir welding parameters on microstructure and mechanical properties of DSS–Cu joints. *Materials Science and Engineering A*, 2017, 693, 111–120.
25. Squillace A, De Fenzo A, Giorleo G, Bellucci F: A comparison between FSW and TIG welding techniques: Modifications of microstructure and pitting corrosion resistance in AA 2024-T3 butt joints. *Journal of Materials Processing Technology*, 2004, 152(1), 97–105.
26. Liu HJ, Shen J J, Zhou L, Zhao Y Q, Liu C, Kuang L Y: Microstructural characterisation and mechanical properties of friction stir welded joints of aluminium alloy to copper. *Science and Technology of Welding and Joining*, 2011, 16(1), 92–98.
27. Pan Y, Zhang D, Liu H, Zhang Z, Li H, Zhuang L, Zhang J: Reducing welding hot cracking of high-strength novel Al–Mg–Zn–Cu alloys based on the prediction of the T-shaped device. *Science and Technology of Welding and Joining*, 2020, 25(6), 483–489.

28. Srinivasa Rao M, Tangudu S S, Perumalla S, Uppda B R, Yandra C, Kambhampati K: Effect of TIG and FSW welding processes on mechanical properties of Al-4.2Mg-0.6Mn-0.4Sc-0.1Zr alloy. *Strojnický Casopis*, 2021, 71(2), 299–304.
29. Mallipudi S R, Shankar TS, Srikanth P, Rao U B, Chandrasekhar Y, Karthikeyan K: Effect of TIG and FSW Welding Processes on Mechanical Properties of Al-4.2Mg-0.6Mn-0.4Sc-0.1Zr Alloy. *Strojnický Časopis - Journal of Mechanical Engineering*, 2021, 71(2), 299–304.
30. Sejc P, Bucany M, Zifcak P: Properties of FSW and MIG Welded Joints of AlSiMgAluminum Alloy, *Strojnický timetable – Journal of Mechanical Engineering*, 2020, 70 (2)pp141 – 152.
31. Vinith B, Dharshan S AD, Aravind S, Singh B K: Friction stir welding evolution, hybrid technologies and shoulder shape. *International Journal on Interactive Design and Manufacturing (IJIDeM)*, 2023, 17(4), 1443–1458.
32. Khan F N, Junaid M, Hassan A A, Baig M N: Effect of pulsation in TIG welding on the microstructure, residual stresses, tensile and impact properties of Ti-5Al-2.5Sn alloy. *Proceedings of the Institution of Mechanical Engineers, Part E: Journal of Process Mechanical Engineering*, 2021, 235(2), 361–370.
33. Das P P, Chakraborty S: Optimization of friction stir welding processes using hybrid-taguchi methods: a comparative analysis. *International Journal on Interactive Design and Manufacturing (IJIDeM)*, 2023, 17(3), 1021–1038.
34. Sunny K T, Korra N N, Vasudevan M, Arivazhagan B: Parameter optimization and experimental validation of A-TIG welding of super austenitic stainless steel AISI 904L using response surface methodology. *Proceedings of the Institution of Mechanical Engineers, Part E: Journal of Process Mechanical Engineering*, 2022, 236(6), 2608–2617.
35. Payak V, Paulraj J, Roy B S, Bhargava M, Das P: A review on recent development in aluminium-copper friction stir welding. *Proceedings of the Institution of Mechanical Engineers, Part E: Journal of Process Mechanical Engineering*, 2023, 1(3), 09544089231158201.
36. Sharma A K, Goyal D, Pabla B S, Saxena K K, Prakash C, Buddhi D: Optimization of friction stir welding parameters for micro alloying of AA6082 alloy. *International Journal on Interactive Design and Manufacturing (IJIDeM)*, 2022, 2960(1).
37. Khan N Z, Siddiquee A N, Khan ZA, Badruddin I A, Kamangar S, Maqbool A: Improvement in joint efficiency with high productivity and narrow weld formation in friction stir welding. *Proceedings of the Institution of Mechanical Engineers, Part E: Journal of Process Mechanical Engineering*, 2022, 236(2), 383–393.
38. Bist A, Saini J S, Sharma V: Comparison of tool wear during friction stir welding of Al alloy and Al-SiC metal matrix composite. *Proceedings of the Institution of Mechanical Engineers, Part E: Journal of Process Mechanical Engineering*, 2021, 235(5), 1522–1533.
39. Buffa G, Fratini L: Friction stir welding of steels: process design through continuum based FEM model. *Science and Technology of Welding and Joining*, 2009, 14(3), 239–246.
40. Sonar T, Ivanov M, Trofimov E, Tingaev A, Suleymanova I: A critical review on solid-state welding of high entropy alloys— processing, microstructural characteristics and mechanical properties of joints. *DefenceTechnology*, 2023, 168(1), 114–165.
41. Wang Q, Zhou X, Wang B, Liu M, Li C, Tan Z, Wu T: Accelerated role of exogenous riboflavin in selective Desulfovibrio desulfuricans corrosion of pipeline welded joints. *Bioelectrochemistry*, 2023, 153, 108469.
42. Dou W, Jia R, Jin P, Liu J, Chen S, Gu T. Investigation of the mechanism and characteristics of copper corrosion by sulfate reducing bacteria. *Corrosion Science*, 2018, 144:237e48.

43. C Razil, A Aangaj: Prediction of relationship between angular velocity to the pitch line velocity (ω/v) on tensile strength of friction stir welded AA2014-T6 Aluminium alloy joints: Angular velocity to pitch line velocity ratio on FSW joints. *Forces in Mechanics*, 2021, 4, 100036.
44. Liu Peng, Li Yajiang, Wang Juan, Geng Haoran: Microstructure characteristics in TIG welded joint of Mg /Al dissimilar materials. *Materials Letters*, 61, 2007, pp. 1288-1291.
45. AC Somasekharan, LE Murr: Characterization of complex, solid-state flow and mixing in the friction-stir welding (FSW) of aluminum alloy 6061-T6 to magnesium alloy AZ91D using color metallography. *Journal of Materials Science*, 41, 2006, pp. 5365-5370.
46. Naga sathwik sridhara S, Chandra siddhardha Allada S, Sharmi Sai, P V Banala, S Subbiah, Marichamy S: Tensile strength performance and optimization of Al 7068 using TIG welding process. *Materials Today: Proceedings*, 2021, 45, 20(17).
47. Yelamasetti B, Adithya G S, Ramadevi R S, Sonia P, Saxena K K, Kumar P N, Eldin S M, Al-kafaji FH K: Metallurgical, mechanical and corrosion behaviour of pulsed and constant current TIG dissimilar welds of AISI 430 and Inconel 718. *Journal of Materials Research and Technology*, 2023, 24, 6652–6664.
48. Tamadon A, Pons D J, Clucas D: Analogue Modelling of Flow Patterns in Bobbin Friction Stir Welding by the Dark-Field/Bright-Field Illumination Method. *Advances in Materials Science*, 2020, 20(1), 56-70.
49. B Yelamasetti, TV Vardhan, GV Ramana: Study of metallurgical changes and mechanical properties of dissimilar weldments developed by interpulse current TIG welding technique. *Proceedings of the Institution of Mechanical Engineers - Part C: Journal of Mechanical Engineering Science*, 2021, 235 (16), pp. 2985-2997.
50. Xuan Y, Yang J, Liu H, Deng J, Wang Y: Microstructure and mechanical properties of Invar36 alloy joints using keyhole TIG welding. *Science and Technology of Welding and Joining*, 2020, 25(8), 712–718.
51. Kumar S A, Sathiya P: Experimental Investigation of the A-TIG Welding Process of Incoloy 800H. *Materials and Manufacturing Processes*, 2015, 30(9), 1154–1159.
52. Dhondt, Matthieu, Aubert, Isabelle, Saintier, Nicolas, Olive, Jean-Marc: Intergranular stress corrosion cracking of friction stir welded nugget on a 2050-T8 aluminum alloy. *Advances in Materials Science*, 2011, 11(3), 43-50.
53. Kusano K, Watanabe H: Recent trends in development of high-efficiency TIG welding; high-deposition TIG welding and ultranarrow-gap TIG welding. *Welding International*, 2002, 16(12), 986–991.
54. Górska J, Przybyła M, Szmul M, Chudzio A, Ładak D: Orbital TIG Welding of Titanium Tubes with Perforated Bottom Made of Titanium-Clad Steel. *Advances in Materials Science*, 2019, 19(3), 55–64.
55. Sridhar SP, Arun Kumar S, Sathiya P: A Study on the Effect of Different Activating Flux on A-TIG Welding Process of Incoloy 800H, *Advances in Materials Science*, 2022, 16(3), 26-37.
56. Dudzik K, Jurczak W: Influence of Friction Stir Welding on Corrosion Properties of Aw-7020M Alloy in Sea Water. *Advances in Materials Science*, 2015, 15(1), 7-13.
57. Zhou D, Xia Y, Gao Z, Bai L, Hu W: Effect of loading conditions on corrosion fatigue process of FSW AA6061-T6 joint in 3.5% NaCl studied by electrochemical noise. *Journal of Materials Research and Technology*, 2023, 24, 9808 9823.
58. Qiu Y, Yang X, Xu J, Li J, Xiang S, Chen Z, Sanders R E: Enhanced mechanical property and corrosion resistance of alloy 5182 FSW joints by Sc and Zr alloying. *Materials Characterization*, 2022, 194, 112412.

59. Raturi M, Bhattacharya A: Electrochemical corrosion of AA6061-AA7075 double sided FSW joints prepared with and without secondary heating. *CIRP Journal of Manufacturing Science and Technology*, 2022, 38, 590–612.
60. Rajendran C, Srinivasan K, Balasubramanian V, Balaji H, Selvaraj P: Feasibility study of FSW, LBW and TIG joining process to fabricate light combat aircraft structure. *International Journal of Lightweight Materials and Manufacture*, 2021, 4(4), 480–490.
61. Emmanuel Sam Franklin D, Vijay SJ, Mohanasundaram S, Nelson R, Hiran Gabriel D J: Investigations on GTAW and FSW of Al6061-ZrB2-Fly ash hybrid metal matrix composites. *Materials Today: Proceedings*, 2021, 47, 6902–6907.
62. Mehdi H, Mishra R S: Effect of friction stir processing on mechanical properties and heat transfer of TIG welded joint of AA6061 and AA7075. *Defence Technology*, 2021, 17(3), 715–727.
63. Kotari S, Punna E, Gangadhar Reddy S M, Venukumar S: Mechanical and micro structural behaviour of flux coated GTAW and FSW joined AA6061 aluminium alloy. *Materials Today: Proceedings*, 2020, 27, 1660–1667.
64. Mehdi H, Mishra RS: Investigation of mechanical properties and heat transfer of welded joint of AA6061 and AA7075 using TIG+FSP welding approach. *Journal of Advanced Joining Processes*, 2020, 1, 100003.
65. Walter V, Weidenmann K A, Schulze V: A Comparison of FSW, BHLW and TIG Joints for Al-Si-Mg Alloy (EN AW-6082 T6). *Procedia CIRP*, 2014, 18, 120–125.
66. Simoncini M, Ciccarelli D, Forcellese A, Pieralisi M: Micro- and Macro- Mechanical Properties of Pinless Friction Stir Welded Joints in AA5754 Aluminium Thin Sheets. *Procedia CIRP*, 2014, 18, 9–14.